LAWRENCE
LIVERMORE
NATIONAL
LABORATORY

UCRL-CONF-227576

High-resolution adaptive optics scanning laser ophthalmoscope with dual deformable mirrors for large aberration correction

D.C. Chen, S. M Jones, D. A. Silva, S. S. Olivier

January 30, 2007

SPIE Photonics West 2007
San Jose, CA, United States
January 20, 2007 through January 25, 2007

High-resolution adaptive optics scanning laser ophthalmoscope with dual deformable mirrors for large aberration correction

Diana C. Chen, Steven M. Jones, Dennis A. Silva, Scot S. Olivier
Lawrence Livermore National Laboratory, 7000 East Avenue, Livermore, CA 94550

ABSTRACT

Scanning laser ophthalmoscopes with adaptive optics (AOSLO) have been shown previously to provide a non-invasive, cellular-scale view of the living human retina. However, the clinical utility of these systems has been limited by the available deformable mirror technology. In this paper, we demonstrate that the use of dual deformable mirrors can effectively compensate large aberrations in the human retina, making the AOSLO system a viable, non-invasive, high-resolution imaging tool for clinical diagnostics. We used a bimorph deformable mirror to correct low-order aberrations with relatively large amplitudes. The bimorph mirror is manufactured by Aoptix, Inc. with 37 elements and 18 μm stroke in a 10 mm aperture. We used a MEMS deformable mirror to correct high-order aberrations with lower amplitudes. The MEMS mirror is manufactured by Boston Micromachine, Inc with 144 elements and 1.5 μm stroke in a 3 mm aperture. We have achieved near diffraction-limited retina images using the dual deformable mirrors to correct large aberrations up to ±3D of defocus and ±3D of cylindrical aberrations with test subjects. This increases the range of spectacle corrections by the AO systems by a factor of 10, which is crucial for use in the clinical environment. This ability for large phase compensation can eliminate accurate refractive error fitting for the patients, which greatly improves the system ease of use and efficiency in the clinical environment.

Keywords: Scanning laser ophthalmoscope; adaptive optics; deformable mirror, off-axis optical aberrations

INTRODUCTION

The invention of confocal scanning laser ophthalmoscope (SLO) [1-2] has brought significant advances in real-time retinal imaging quality in terms of improved imaging resolution and increased light collection efficiency. The use of adaptive optics (AO) in the scanning laser ophthalmoscope [3-16] to correct ocular aberrations has further increased the imaging quality by reducing the wavefront errors in the optical paths. In an AO SLO, the ocular aberrations of the test subjects are measured by a wavefront sensor. The measured wavefront errors are then used to adjust the shape of a deformable mirror (DM) until the wavefront aberrations are minimized.

Population studies have shown that many people have both low-order aberrations with large amplitudes and high-order aberrations with lower amplitudes [17-19]. For these subjects, current technology cannot deliver the phase compensation needed using a single DM in a compact AOSLO system. To address the issue, we investigated the use of multiple deformable mirrors in the AOSLO. Specifically, we employed one DM to correct low-order aberrations with relatively large amplitudes and a second DM to correct high-order aberrations with lower amplitudes. Collectively, the dual deformable mirrors provided the necessary real-time ocular aberration corrections to achieve diffraction-limited *in-vivo* retinal images.

In this paper, we will discuss the development the imaging results of the dual-deformable mirror adaptive optics scanning laser ophthalmoscope system for large aberration compensation. We will also discuss the limitation of the current system and further improvements of the future system.

METHODS

Figure 1 shows the optical system layout of the two-deformable-mirrors adaptive optics scanning laser ophthalmoscope. Incoming illumination light is coupled into a single-mode fiber, then collimated and relayed by telescopes to the two DMs, horizontal and vertical scanners, and finally the eye. The scattered light from the retina follows the same optical paths as the incoming light, but along the inverse direction and then is coupled into a photomultiplier tube (PMT). The high-resolution retinal image is thus detected. The wavefront sensor corrects the aberrations in both incoming illumination path and outgoing imaging path so that a diffraction limited image is obtained.

Two light sources, superluminescent diodes (SLD) from Superlum SLD-371-HP2-DBUT-SM-PD (λ_0 = 843.3 nm, $\Delta\lambda$ = 48.3 nm, P=18 mW) and SLD-261-HP1-DIL- SM-PD (λ_0 = 682 nm, $\Delta\lambda$ = 9.6 nm, P= 5 mW) are used in the AOSLO. Both light sources are fiber coupled. A compact package, consisting of a FC single mode fiber connector, an x-y-z stage for adjusting the collimation lens, an achromatic lens, and a system aperture, delivers collimated light of the desired wavelength into the AOSLO. The use of different wavelengths is accomplished by switching the incoming optical fibers to the light delivery package.

Wavefront sensing and the detection paths in the AOSLO are designed to share the same light path as far as possible to minimize the non-common path errors. The wavefront error is measured with a Shack-Hartmann wavefront sensor consisting of a 20x20 lenslet array (Adaptive Optics Associates, 0500-30-S-A, 500 um pitch, 30 mm focal length) and a CCD camera (Dalsa 1M60 CCD CameraLink) at its focal plane.

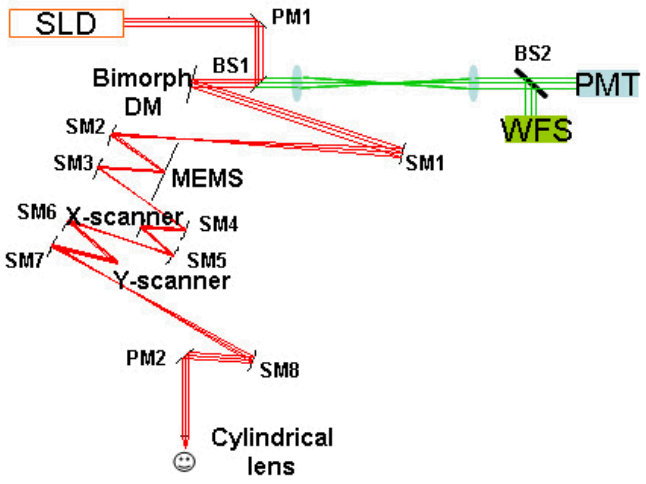

Fig.1. Optical system layout of the dual DM adaptive optics scanning laser ophthalmoscope. SLD, Superluminescent Laser Diode; BS, Beam splitter; PM, Plane Mirror: SM, Spherical Mirror; WFS, Wavefront Sensor; PMT, Photomultiplier Tube

The focused beam is scanned on the retina in a raster pattern with a horizontal scanner (Electro-Optics Products Corp., SC-30 resonate scanner, 14 kHz, 6°) and a vertical scanner (Cambridge Technology, 6220M40 galvanometric scanner, ±20°). The two scanners are separated by a relay telescope designed to make them optically conjugate to each other and to the entrance pupil of the eye. This minimizes the movement of the scanning beam at the pupil, which is important for proper functioning of the AOSLO system. The optical design is optimized for a field of view of 2.9° x 2.9° (optical scan angle) for a 6 mm circular eye pupil. The scanned image corresponds to a 0.9 mm x 0.9 mm area on retina.

Two DMs are phased conjugated to each other and also to the pupil plane of the eye, which allows phase cascading for the ocular aberration correction. A bimorph mirror (Manufactured by Aoptix, Inc. with 37 elements and 18 μm stroke in a 10 mm aperture, see Fig. 2(a)) is used to correct large-stroke, low-order aberrations. A MEMS mirror (Manufactured by Boston Micromachine, Inc with 144 elements and 1.5 μm stroke in a 3 mm aperture, see Fig. 2(b)) is used to correct low-stroke, high-order aberrations.

The wavefront compensation in the AOSLO is accomplished using a two-step process. In the first step, the AO-computer reads the measured wavefront aberration in the subject's eye from the Shack-Hartmann wavefront sensor and the bimorph mirror is reshaped to minimize the wavefront aberrations while the MEMS mirror is still. In the second step, the bimorph mirror is held "static", and the residual wavefront aberrations are measured by the Shack-Hartmann wavefront sensor and the MEMS DM is reshaped to further minimize the wavefront aberrations [14-17].

Fig. 2(a)

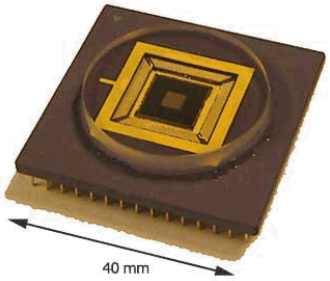

Fig. 2(b)

Fig .2 Deformable mirrors used in the AOSLO system (a) The bimorph deformable mirror, manufactured by Aoptix Technologies. The bimorph mirror has 35 actuators with 10 mm in diameter clear optical aperture, and 18 μm stroke. (b) The MEMS deformable mirror, manufactured by Boston Micromachines Corp. The MEMS mirror has 144 actuators, with 3.3 mm x 3.3 mm optical clear aperture and 1.5 μm stroke.

The bimorph mirror is used to compensate the prescription aberrations such as defocus and astigmatism so that the actuators of MEMS are not saturated for high-order aberration corrections. In this way, trial lenses or Badal optometers can be eliminated. This brings the benefits of increasing optical throughput, eliminating undesired back reflections and avoiding moving parts to the AOSLO system.

After the wavefront compensation with deformable mirrors, the light coming from the retina is focused through a confocal pinhole and detected with a GaAs photomultiplier tube (H7422-50, Hamamatsu). All the optical components are assembled on a 2'x3' optical breadboard, mounted on a cart with wheels so that the ophthalmoscope can be easily moved to different offices in an ophthalmology clinic.

RESULTS

The dual-deformable-mirrors AOSLO is used in clinical settings to image both healthy and diseased eyes with different amount of ocular aberrations. Fig. 3 shows the retinal images acquired from an emmetropic eye (0D) at the same retinal position with and without aberration corrections using the dual deformable mirrors (a) without AO correction (b) first DM turned on (Bimorph) (c) second DM turned on (MEMS). The images were taken with the 843 nm SLD. The imaging position was at the retinal location of 3° Nasal and 3° Superior and the field of view is 1.1° x 1.1°.

The RMS wavefront error without AO was 248 nm over 6 mm pupil, and it was reduced to 90 nm when the first deformable mirror was turned on. The MEMS DM further reduced the RMS wavefront error to 48 nm. The AO corrected images showed higher resolution and increased brightness as the RMS wavefront error decreased with the AO correction.

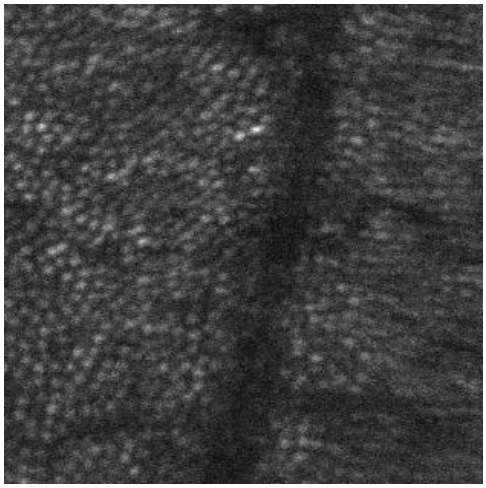

Fig. 3(a)

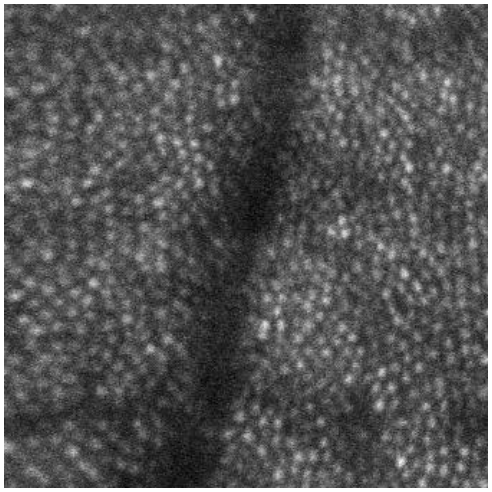

Fig. 3(b)

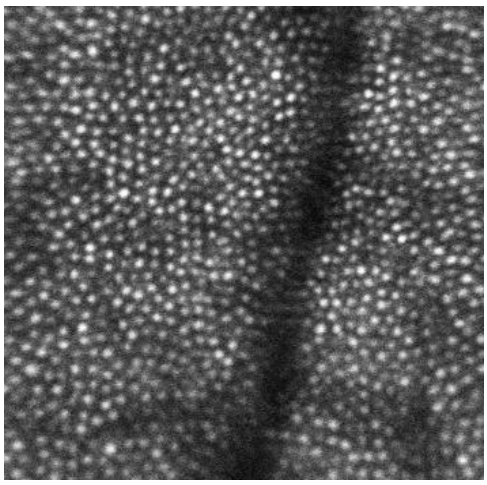

Fig. 3(c)

Fig. 3 Retina images from an emmetropic eye with dual AO corrections taken at 3° Nasal/ 3° Superior Retina, 1.1° x 1.1° scanning angle at wavelength of 843 nm.(a) without AO correction. (b) with closed-loop operation of the bimorph DM (c) with closed-loop operation of the MEMS DM

Fig. 4 and Fig. 5 show the retina images with dual AO corrections taken at 3° Nasal/ 3° Superior Retina, 1.1° x 1.1° scanning angle at wavelength of 840 nm with and without aberration corrections using the dual deformable mirrors. Fig. 4 shows the results of the test subject with +3D defocus. The RMS wavefront error was reduced to 240 nm when the bimorph mirror was turned on and further reduced to 60 nm when the MEMS was in operation. Fig. 5

shows the results of the test subject with +3D cylindrical aberration along x-direction. The RMS wavefront error was reduced to 360 nm when the bimorph mirror was turned on and further reduced to 70 nm when the MEMS was in operation. With the use of bimorph deformable mirror to compensate the low-order aberrations with large magnitudes and MEMS to compensate high-order with small magnitudes, diffraction-limited high-resolution images are acquired effectively.

The capability of large phase compensation of the dual-DM AOSLO greatly increases the spectacle correction range of existing AO systems by a factor of 10, from ±1/4D to ±3D. An autorefractor can quickly fit a patient's prescription to within a diopter, but no necessarily to within 1/4D. Patients with very large refractive error may still need a coarse adjustment using a trial lens or optometer in order to fall within the capture range of the bimorph mirror, but the large range of phase compensation make the coarse fitting trivial. Clinicians do not have to spend time to make sure that the refractive correction is highly accurate. This would drastically speeds up the whole imaging process and makes the use of the system wieldy in a clinical environment

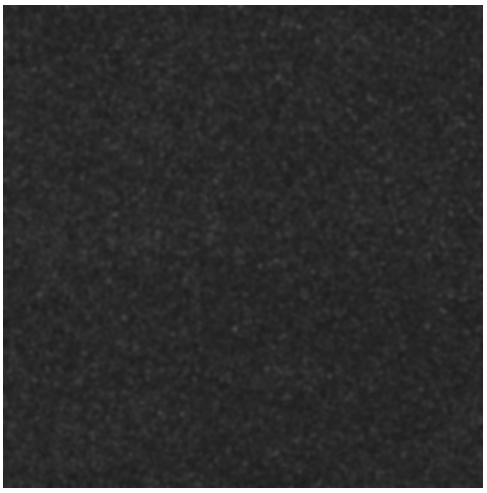

Fig. 4(a)

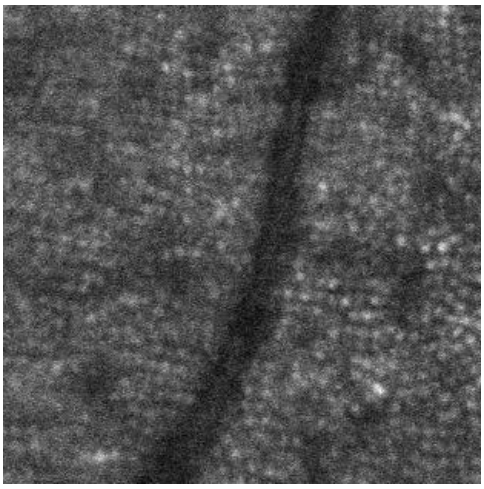

Fig. 4(b)

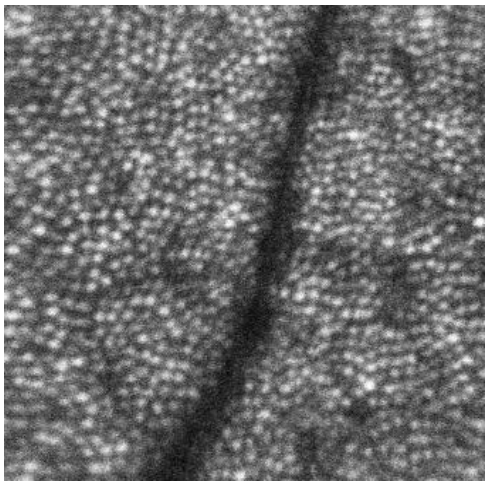

Fig. 4 (c)

Fig. 4 Retina images with dual AO corrections taken at 3° Nasal/ 3° Superior Retina, 1.1° x 1.1° scanning angle at wavelength of 840 nm. Test subject has +3D defocus . (a) without AO correction. (b) with closed-loop operation of the bimorph DM (c) with closed-loop operation of the MEMS DM

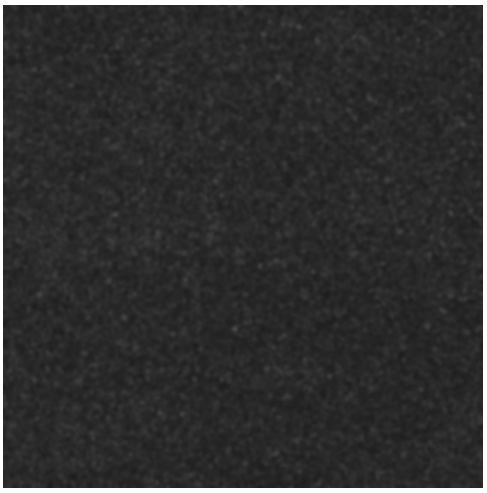

Fig. 5(a)

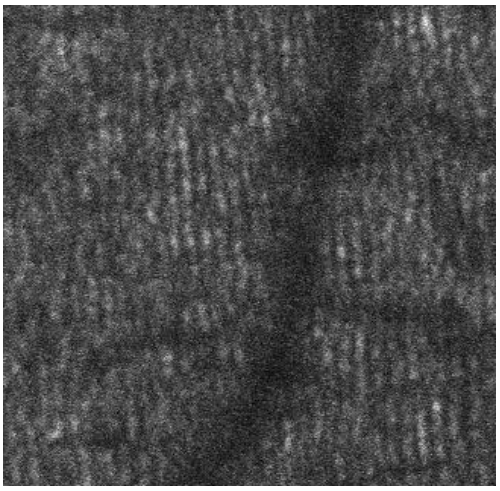

Fig. 5(b)

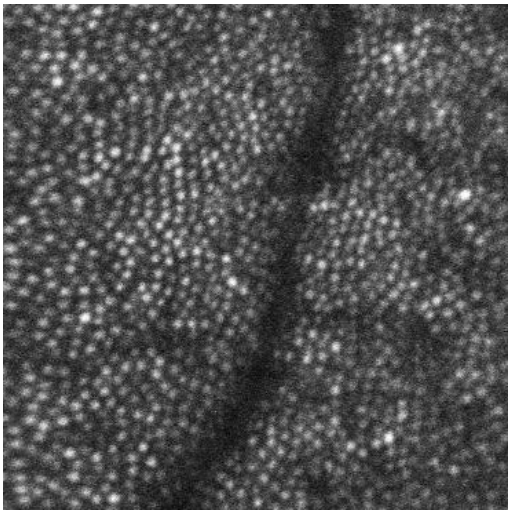

Fig. 5 (c)

Fig. 5 Retina images with dual AO corrections taken at 3° Nasal/ 3° Superior Retina, 1.1° x 1.1° scanning angle at wavelength of 840 nm. Test subject has +3D cylindrical aberration along x-direction. (a) without AO correction. (b) with closed-loop operation of the bimorph DM (c) with closed-loop operation of the MEMS DM

LIMITATIONS OF THE CURRENT SYSTEM

Limitation from the deformable mirror

The magnitude of the ocular aberrations which can be compensated by the AOSLO system is determined by the maximum stroke of the deformable mirror. The largest defocus the bimorph can compensated can be easily calculated using the equation,

$$\Phi = \frac{16\Delta}{d^2}$$

where Φ is the defocus in diopter, Δ is the total stroke of the bimorph deformable mirror in μm and d is the diameter of the bimorph deformable mirror in mm.
The bimorph mirror from Aoptix Technologies has the stroke of 18 μm with 10 mm diameter. The maximum defocus or cylindrical aberration it can correct is limited to ± 3D. Larger amount of defocus or cylindrical aberration requires a deformable mirror with larger strokes for effect compensation. The largest amount of displacement needed can be calculated by

$$\Delta = \frac{\Phi d^2}{16}$$

where again Φ is the defocus in diopter, Δ is the total stroke of the bimorph deformable mirror in μm and d is the diameter of the bimorph deformable mirror in mm.

Limitation from the optical system design

We have demonstrated experimentally that the AOSLO system work well up to ± 3D in the previous session. However, beyond that the relay aberrations will degrade the performance of the AO system due to pupil aberration and distortion. In the future, new AO mirror technology may be used that can correct more aberrations, and this requires a better relay optic design.

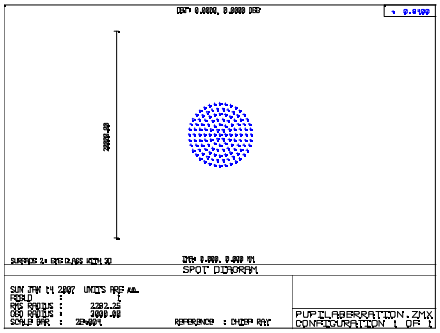

Fig. 6(a)

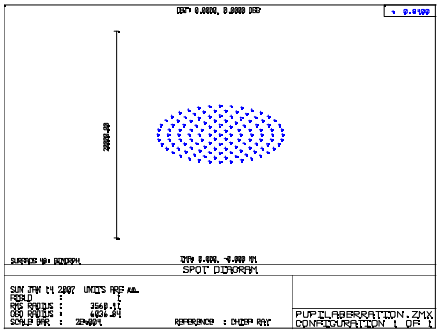

Fig. 6(b)

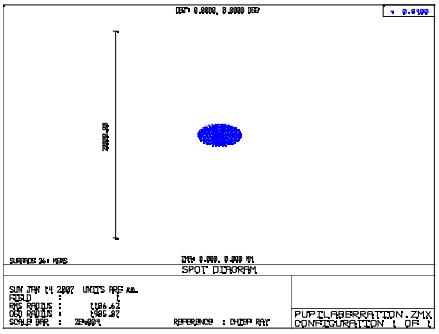

Fig. 6 (c)

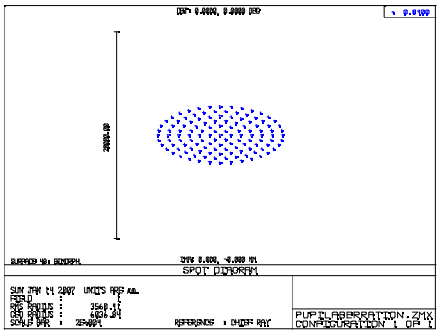

Fig. 6(d)

Fig. 6 Pupil images with a defocus of 5D at the eye (a) at the eye pupil (b) at the bimorph mirror (c) at the MEMS (d) at the wavefront sensor

Adaptive optics systems typically use optical relays that simultaneously image the science field to be corrected and also a set of pupil planes conjugated to the deformable mirrors of the system. Ocular aberration correction is achieved by placing the Shack-Hartmann wavefront sensor and the two DMs at planes conjugate to the pupil of the eye. Each component is placed at the image plane of an afocal relay telescope. Fig. 6 illustrates the pupils at the planes of the eye, the bimorph mirror, MEMS and wavefront sensor with a defocus of 5D at the eye. Pupils at different conjugated planes are evidently distorted and aberrated at the deformable mirrors and wavefront sensors, which would severely degrade the effectiveness of AO compensation.

If all the optical relays are perfectly aberration free, all the pupils should be circular with no aberrations or distortions. This indicates that optical relay creates the aberrations to the AOSLO system. To reduce back reflections, spherical mirrors, instead of lenses, are used in the afocal telescope designs. This has the additional benefit of eliminating chromatic aberrations in the system, but it also creates additional aberrations such as spherical, coma and astigmatism[20] .

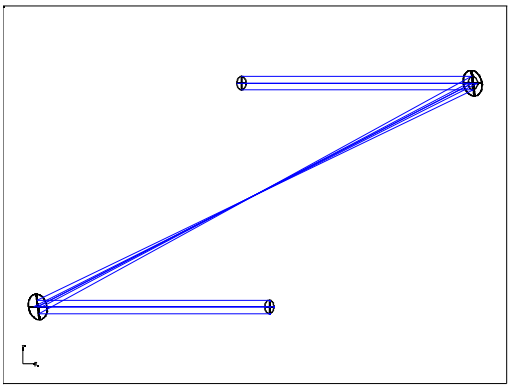

Fig. 7(a)

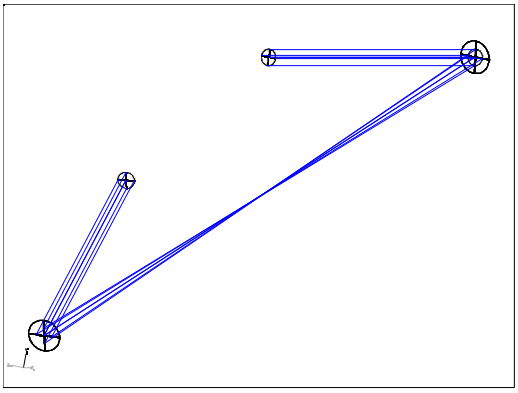

Fig.7(b)

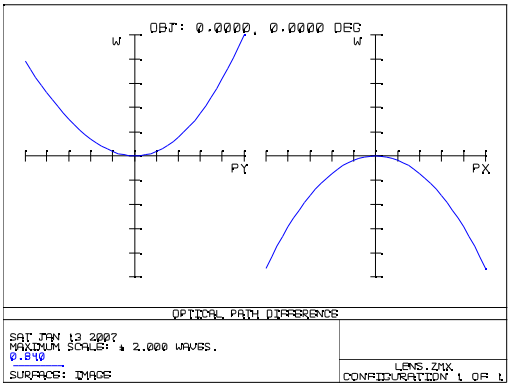

Fig. 7(c)

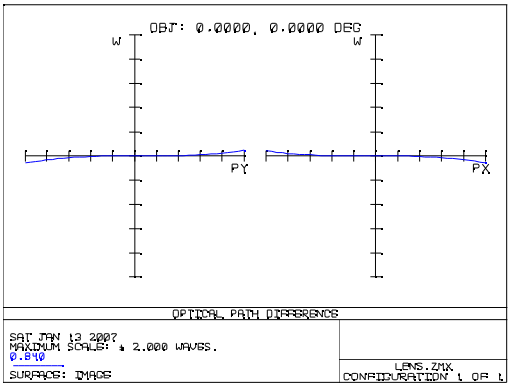

Fig. 7(d)

Fig. 7. the optical design of a 1:1 afocal telescope with the tilt angle of 10°, a radius of curvature of 500 mm for both mirrors, and entrance pupil diameter of 10mm. (a) the afocal telescope with both mirrors tilting in the same plane. (b) the afocal telecope with two mirrors tilting in the orthogonal planes. (c) optical path difference diagram of design Fig. 7(a). (d) optical path difference diagrams of design Fig. 7(b).

Detailed analysis of the optical system shows that the ratio of the spherical aberration, coma and astigmatism of a spherical mirror in the afocal telescope is given by

$$\textbf{Spherical/Coma/Astigmatism} = 1: 4\theta F: (4\theta F)^2,$$

where θ is the tilt angle of the spherical mirror and F is the F number of the system.
For a mirror with a radius of 500 mm , entrance pupil diameter of 10 mm and tilt angle of 5°, the ratio of Spherical/Coma/Astigmatism = $1/8.7/8.7^2$ = 1:8.7:75.7. So clearly astigmatism is the dominating aberration.

There are many ways to correct the astigmatism caused by the spherical mirror such as adding wedges or flat plates, or adding cylindrical surfaces or lenses. The simplest way is to tilt the second spherical mirror of the afocal telescope in the orthogonal planes to let the two spherical mirrors cancel the astigmatism introduced by a single mirror. Tilt the second mirror in the same plane, but in the opposite direction would double the astigmatism instead of canceling each other out.

Fig. 7 shows the optical design of a 1:1 afocal telescope with the tilt angle of 10°, a radius of curvature of 500 mm for both mirrors, and entrance pupil diameter of 10mm. Fig 7(a) shows the afocal telescope with both mirrors tilting in the same plane and Fig.7(b) shows the afocal telecope with two mirrors tilting in the orthogonal planes. Fig. 7(c) and Fig. 7(d) show the optical path difference diagrams of the two designs. The RMS values of the two designs are 0.75 waves and 0.018 waves. Clearly, telescope with the orthogonal tilting mirrors effectively minimize the aberrations and a diffraction-limited relay telescope is achieved. The same principle can be applied to all the relay telescopes in the AOSLO system. This can effectively minimize the pupil aberrations among the image relays, and ensure the performance of the AO operation when large ocular aberration compensation are needed

CONCLUSION

We have achieved near diffraction-limited retina images using the dual deformable mirrors to correct large aberrations up to ±3D of defocus and ±3D of cylindrical aberrations with test subjects. This increases the range of spectacle corrections by the AO systems by a factor of 10 and effectively eliminates accurate refractive error fitting of the patients, which is crucial for use in a clinical environment. The dual-AOs significantly improve lateral resolution, contrast and brightness and potentially eliminate the trial lenses for most patients. This greatly improves the system ease of use and efficiency in a clinical environment.

ACKNOWLEDGEMENTS

This research was supported by the NIH grant EY014365 and performed under the auspices of the U.S. Department of Energy by University of California, Lawrence Livermore National Laboratory under Contract W-7405-Eng-48. All testing and imaging of subjects with this system was performed at the UC Davis Medical Center in collaboration with Jack Werner's group. We particularly benefited from technical discussions from Austin Roorda's group at UC Berkeley.

REFERENCES

1. R. Webb and G. Hughes, "Scanning laser ophthalmoscope," IEEE Trans. on Bio. Eng. **28**, 488-492 (1981)
2. R. Webb, G. Hughes, and F. Delori, "Confocal scanning laser ophthalmoscope,", Appl. Opt. **26**, 1492-1499 (1987)
3. A. Dreher, J. Bille, and R. Weinreb, "Active optical depth resolution improvement of the laser tomography scanner", Appl. Opt. **28,** 804-808 (1989)
4. J. Liang, D. Williams, and D. Miller, "Supernormal vision and high-resolution retinal imaging through adaptive optics", J/ Opt. Am. A **14**, 2884-2892 (1997).
5. A. Roorda, F. Romero-Borja, W. Donnelly, H. Queener, T. Herbert, and M. Campbell, "Adaptive optics scanning laser ophthalmoscopy", Opt. Exp. **10**. 405-412 (2002).
6. Y. Zhang, S. Poonja, and A. Roorda, "Adaptive optics scanning laser ophthalmoscope using a micro-electro-mechanical (MEMS) deformable mirror," Proc. of SPIE **6138**, 0Z1-0Z11 (2006)
7. H. Hofer, L. Chen, G. Yoon, B. Singer, Y. Yamauchi, and D. Williams, "Improvement in retinal image quality with dynamic correction of the eye's aberration," Optics Express, **8**, 631-643 (2001)
8. F. Vargas-Martin, P. Prieto, and P. Artal, "Correction of the aberrations in the human eye with a liquid-crystal spatial light modulator: limits to performance", J. Opt. Am. A **15,** 2552-2562 (1998).

9. T. Bifano, J. Perreault, P. Bierden, and C. Dimas, "Michromachined deformable mirrors for adaptive optics," Proc. of SPIE **4825**, 10-13 (2002)
10. G. Yoon, "Wavefront sensing and diagnostic users", *Adaptive Optics for Vision Science*, (Wiley & Sons, 2006), 63-81
11. J. Liang, B. Grimm, S. Goelz, J. Bille, "Objective measurement of wavefront aberrations of the human eye with the use of a Hartmann-Shack wave-front sensor," J. Opt. Am. A. **11**, 1949-1957, (1994)
12. D. Horsley, H. Park, S. Laut and J. Werner, "Characterization for vision science applications of a bimorph deformable mirror using phase-shifting interferometry", SPIE **5688,** 133-144 (2005)
13. S. Hu, B. Xu, X. Zhang, J. Hou, J. Wu and W. Jiang, "Double-deformable-mirror adaptive optics system for phase compensation", Appl. Opt. **45,** 2638-2642 (2006)
14. J. Barchers, "Closed-loop stable control of two deformable mirrors for compensation of amplitude and phase fluctuations," J. Opt. Am. A **19**, 926-945 (2002)
15. A. Roorda, F. Romero-Borja, W. Donnelly, H. Queener, T. Herbert, and M. Campbell, "Adaptive optics scanning laser ophthalmoscopy", Opt. Exp. **10**. 405-412 (2002).
16. J. Liang, D. Williams, and D. Miller, "Supernormal vision and high-resolution retinal imaging through adaptive optics", J/ Opt. Am. A **14**, 2884-2892 (1997).
17. J. Porter, A. Guirao, I. Cox and D. Williams, "Monochromatic aberrations of the human eye in a large populations," J. Opt. Am. A. **18**, 1793-1803, (2001)
18. L. Thibos, X. Hong, A. Bradley and X. Cheng, "Statistical variation of aberration structure and image quality in a normal population of healthy eyes," J. Opt. Am. A. **19**, 2329-2348 (2002)
19. A. Elsner, "Fundamental properties of the retina", *Adaptive Optics for Vision Science*, (Wiley & Sons, 2006), 205-234
20. W. T. Welford, "Aberrations of optical systems", (Adam Hilger, 1986)